The Plant Cell, Vol. 11, 1381–1392, August 1999, www.plantcell.org © 1999 American Society of Plant Physiologists

RESEARCH ARTICLE

Cloning and Functional Characterization of an Arabidopsis Nitrate Transporter Gene That Encodes a Constitutive Component of Low-Affinity Uptake

Nien-Chen Huang,[a] Kun-Hsiang Liu,[a,b] Hau-Jan Lo,[a] and Yi-Fang Tsay[a,1]

[a] Institute of Molecular Biology, Academia Sinica, Taipei, Taiwan
[b] Graduate Institute of Life Sciences, National Defense Medical Center, Taipei, Taiwan

The Arabidopsis *CHL1* (*AtNRT1*) gene encodes an inducible component of low-affinity nitrate uptake, which necessitates a "two-component" model to account for the constitutive low-affinity uptake observed in physiological studies. Here, we report the cloning and characterization of a *CHL1* homolog, *AtNRT1:2* (originally named *NTL1*), with data to indicate that this gene encodes a constitutive component of low-affinity nitrate uptake. Transgenic plants expressing antisense *AtNRT1:2* exhibited reduced nitrate-induced membrane depolarization and nitrate uptake activities in assays with 10 mM nitrate. Furthermore, transgenic plants expressing antisense *AtNRT1:2* in the *chl1-5* background exhibited an enhanced resistance to chlorate (7 mM as opposed to 2 mM for the *chl1-5* mutant). Kinetic analysis of *AtNRT1:2*-injected Xenopus oocytes yielded a K_m for nitrate of ~5.9 mM. In contrast to *CHL1*, *AtNRT1:2* was constitutively expressed before and after nitrate exposure (it was repressed transiently only when the level of *CHL1* mRNA started to increase significantly), and its mRNA was found primarily in root hairs and the epidermis in both young (root tips) and mature regions of roots. We conclude that low-affinity systems of nitrate uptake, like high-affinity systems, are composed of inducible and constitutive components and that with their distinct functions, they are part of an elaborate nitrate uptake network in Arabidopsis.

INTRODUCTION

Ion uptake during rapid vegetative growth can consume up to 36% of total respiratory energy cost (ATP) (Werf et al., 1988). A significant portion of this demand is devoted to nitrogen acquisition, for which nitrate from soil is a major supplying source. Extensive studies have hence focused on the kinetics and, more recently, the molecular genetics of nitrate uptake (Glass and Siddiqi, 1995; Wirén et al., 1997; Crawford and Glass, 1998; Daniel-Vedele et al., 1998).

Two kinetically distinct nitrate uptake systems, the high-affinity transport system (HATS) and the low-affinity transport system (LATS), have been identified. Depending on the plant species, the HATS has a K_m of ~5 to 100 μM, whereas the LATS shows linear kinetics or K_m values in the millimolar range (Doddema and Telkamp, 1979; Goyal and Huffaker, 1986; Lee and Drew, 1986; Siddiqi et al., 1990; Aslam et al., 1992; Meharg and Blatt, 1995). In general, the LATS has a larger capacity than does the HATS. For example, it was reported that in Arabidopsis, the uptake rate at 10 mM nitrate (~24 μmol hr^{-1} g^{-1} fresh weight) is 24 times higher than is the V_{max} of the HATS (~1 μmol hr^{-1} g^{-1} fresh weight) (Touraine and Glass, 1997). Thus, whereas the HATS is important for nitrogen acquisition when external nitrate concentration is low, the LATS is required for mass amounts of nitrogen acquisition. The latter may be more important for growing crops, because nitrate is difficult to retain and its concentration fluctuates significantly in arable soil.

In response to nitrate induction, the HATS can be further divided into two components, one that is inducible (iHATS) and one that is constitutive (cHATS). The cHATS accounts for the residual high-affinity nitrate uptake activity observed in plants never exposed to nitrate, whereas when exposed to nitrate, the iHATS with its higher capacity is induced after only a few hours (Lee and Drew, 1986; Behl et al., 1988; Hole et al., 1990; Siddiqi et al., 1990; Aslam et al., 1992). Recent reports suggest that members of the nitrate transporter *NRT2* family, which is distinct from the *NRT1* family comprising *CHL1* (*AtNRT1*) and its homologs, are involved in nitrate uptake via the iHATS (Trueman et al., 1996a, 1996b; Quesada et al., 1997; Krapp et al., 1998).

Different from the HATS, the LATS has long been thought to comprise only a constitutive component (Glass and Siddiqi, 1995). However, functional characterization of *CHL1*

[1] To whom correspondence should be addressed. E-mail mbyftsay@ccvax.sinica.edu.tw; fax 886-2-2782-6085.

showed that it is a nitrate-inducible gene that encodes a nitrate transporter (Tsay et al., 1993) involved in low-affinity uptake (Huang et al., 1996). This conclusion is based on the reduced low-affinity nitrate uptake activity of *chl1* mutants (Doddema et al., 1978; Doddema and Telkamp, 1979; Huang et al., 1996; Touraine and Glass, 1997), recovery of the uptake defect in a *chl1* mutant expressing the *CHL1* cDNA driven by the cauliflower mosaic virus 35S promoter, and in vitro functional assays using *CHL1*-expressed Xenopus oocytes (Huang et al., 1996). This conclusion is further supported by the results of in situ hybridization experiments that demonstrate that *CHL1* mRNA is expressed in the epidermis, cortex, or endodermis of roots (Huang et al., 1996). These data regarding *CHL1* are inconsistent with the preponderant model of a single, constitutive component for low-affinity nitrate uptake. Consequently, a "two-component" model analogous to the iHATS and cHATS for the LATS was proposed (Huang et al., 1996). In this model, the iLATS (for inducible LATS) is mediated by *CHL1* and the cLATS (for constitutive LATS) by a distinct and previously unidentified gene.

We describe here the cloning and characterization of a *CHL1* homolog from Arabidopsis, *AtNRT1:2*. Results from both in vivo and in vitro uptake measurements, nitrate-induced membrane depolarization, and in situ hybridization experiments indicate that *AtNRT1:2* encodes a nitrate transporter that functions as the cLATS, thereby confirming the two-component model. In addition, the unique properties of *AtNRT1:2* provide new insights into the nitrate uptake mechanisms of higher plants.

RESULTS

Cloning and Sequence Analysis of the *AtNRT1:2* Gene

AtNRT1:2 was identified by a homology search, using the *CHL1* sequence against the expressed sequence tag (EST) database of Arabidopsis. In addition to the original EST clone (p*AtNRT1:2-1*; clone number YAP049), we isolated a second 2-kb cDNA clone (p*AtNRT1:2-2*) by screening an Arabidopsis cDNA library constructed in the λYES vector (Elledge et al., 1991). Sequence analysis of these two clones indicated that they contain an open reading frame encoding a 585–amino acid protein with a predicted molecular mass of 64 kD. Hydropathy analysis of the deduced amino acid sequence shown in Figure 1A suggests that AtNRT1:2 contains 12 putative transmembrane domains, with a long loop comprising many charged residues separating the first six transmembrane domains from the second six.

The deduced amino acid sequence of AtNRT1:2 is 36% identical to that of CHL1. As shown in Figure 1B, the alignment beginning at the first methionine between CHL1 and AtNRT1:2 indicates that although the 5′ untranslated region in p*AtNRT1:2-1* is very short (11 bases long), this clone contains the full coding sequence. This was further confirmed by sequencing a genomic clone in this region (data not shown). The sequence of this genomic clone revealed no in-frame methionine upstream of the putative translation initiation site. In AtNRT1:2, there is one potential N-linked glycosylation site (Asn-X-Ser/Thr) at position 49 to 51 between

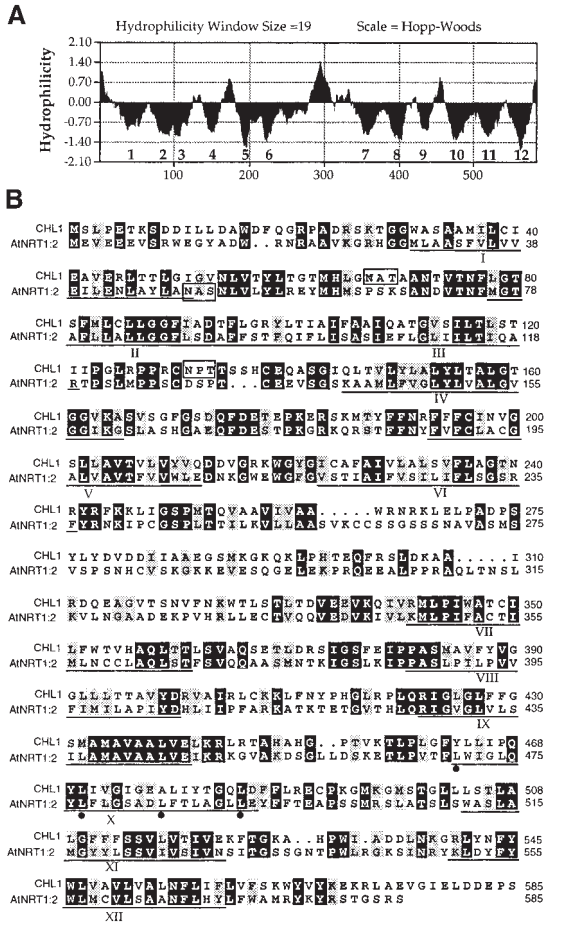

Figure 1. Hydropathy Profile of AtNRT1:2 and Sequence Alignment between AtNRT1:2 and CHL1.

(A) The hydropathy profile of AtNRT1:2 was determined by the Hopp–Woods method (Hopp and Woods, 1981), using a window of 19 amino acid residues. The 12 putative transmembrane domains are numbered.

(B) Sequence alignment between AtNRT1:2 and CHL1 was created using the Genetics Computer Group program (version 9.1; Genetics Computer Group, Madison, WI) with a gap penalty of 12 and a gap length penalty of 4. The putative transmembrane regions are underlined and numbered. Potential sites for N-glycosylation in AtNRT1:2 and CHL1 are boxed, and the four leucine residues encompassing a putative leucine zipper in the putative 10th transmembrane domain of AtNRT1:2 are marked by solid circles. Black and shaded regions represent identical residues and conservative substitutions, respectively. The GenBank accession number for AtNRT1:2 is AF073361. Dots represent gaps inserted to optimize the alignment.

the first and second putative membrane-spanning domains (Figure 1B). In addition, a heptad repeat of four leucine residues ("leucine zipper"; $LX_6LX_6LX_6L$) is found in a region that coincides with the tenth putative transmembrane domain (Figure 1B).

Functional Analysis of *AtNRT1:2* in Xenopus Oocytes

To determine whether *AtNRT1:2* encodes a nitrate transporter, in vitro–synthesized *AtNRT1:2* complementary RNA (cRNA) was injected into Xenopus oocytes for functional assay. As shown in Table 1, like *CHL1*-injected oocytes (Tsay et al., 1993), *AtNRT1:2*-injected oocytes responded to nitrate at pH 5.5 by depolarizing the membrane potential with an inward current across the plasma membrane of the oocytes. This inward current was elicited by nitrate and not by a change in pH, because in the absence of nitrate, shifting from pH 7.4 to pH 5.5 resulted in no response or a small outward current (~5 nA) in both *AtNRT1:2*- and water-injected oocytes (data not shown). The inward current change elicited by nitrate at pH 5.5 in *AtNRT1:2*-injected oocytes (37.4 ± 20.4 nA) was ~10 times larger than that in water-injected controls (3.9 ± 3.8 nA). The current into *AtNRT1:2*-injected oocytes in response to nitrate is pH dependent (e.g., the current elicited by nitrate at pH 7.4 is ~23% of the current elicited by nitrate at pH 5.5; data not shown). Because in addition to a proton, the only cation in the external solution is 0.6 mM calcium, the positive inward current in response to nitrate and its pH dependence support the notion that AtNRT1:2 functions as a proton-coupled nitrate transporter.

The sequences of several dipeptide transporters, including AtPTR2B (Frommer et al., 1994; Rentsch et al., 1995; Song et al., 1996) from Arabidopsis, are related to that of CHL1, and together they form a novel cotransporter family called POT (for proton-dependent oligopeptide transporter; Paulsen and Skurray, 1994) or PTR (for peptide transporter; Steiner et al., 1995). To determine whether AtNRT1:2 is also capable of mediating the uptake of dipeptide, the same *AtNRT1:2*-injected oocytes were exposed to nitrate and the dipeptide Gly-Gly at pH 5.5. For the three oocytes tested at −60 mV, the inward current elicited by nitrate was 36 ± 9.5 nA; in contrast, a small current (−3.6 ± 11.7 nA) close to the background level of responses found in water-injected oocytes was observed with dipeptide Gly-Gly (data not shown). In addition to Gly-Gly, the positively charged dipeptide Ala-His, the negatively charged dipeptide Ala-Asp, and a neutral dipeptide (Ala-Leu) elicited no response in *AtNRT1:2*-injected oocytes at any of the voltages tested from 0 to −160 mV, whereas nitrate induced significant voltage-dependent currents, as expected for an electrogenic transporter (Figure 2).

Recently, histidine uptake activities have been reported for two members of the PTR family, BnNRT1;2 from Brassica (Zhou et al., 1998) and PHT1 (for peptide/histidine transporter) from rat (Yamashita et al., 1997). In this study, to investigate whether histidine is a substrate of AtNRT1:2, the oocytes examined for nitrate uptake were also assayed with 10 mM histidine at pH 5.5 or 8.5. Either none or only very small responses close to the background level of water-injected controls were observed (Figure 2). Similar results were obtained in three independent oocytes isolated from two different frogs. These data indicate that AtNRT1:2 is a nitrate transporter with little, if any, uptake activity for either histidine or the dipeptides tested.

As shown in Figure 3, the amplitude of the inward current elicited by nitrate at pH 5.5 was concentration dependent. By fitting the currents into a Lineweaver–Burk plot, the K_m values obtained in five independent oocytes were 4.9 (shown in Figure 3), 7.4, 6.7, 7.9, and 2.6 mM, which yielded an average value of 5.9 ± 1.9 mM.

It has been shown that K_m values derived from similar oocyte analyses are voltage dependent for a number of transporters, including two CHL1 homologs, the nitrate transporter BnNRT1;2 from Brassica and the peptide transporter PepT1 from humans (Boorer et al., 1994, 1996; Mackenzie et al., 1996; Zhou et al., 1998). However, in these reports, the magnitude of maximal changes in the K_m measured between −60 mV and −150 or −200 mV is less than fivefold. Such a magnitude of change would project a K_m for AtNRT1:2 at low, plant-relevant membrane potentials (e.g., −200 mV) that remains in the millimolar range corresponding to low-affinity nitrate uptake. These oocyte data, taken together with the observation that only low-affinity but not high-affinity nitrate uptake activity is reduced in antisense *AtNRT1:2* plants (see below), suggest that *AtNRT1:2* encodes a low-affinity nitrate transporter.

Table 1. Membrane Potential and Whole-Cell Current Measurements of Oocytes Exposed to 10 mM Nitrate, pH 5.5

Oocyte Injection	Inward Currents Elicited[a] (nA)	Oocytes Tested[b]	Membrane Potential Depolarized[a] (mV)	Oocytes Tested[b]
AtNRT1:2 cRNA	37.4 ± 20.4	*n* = 13	13.8 ± 5.4	*n* = 4
CHL1 cRNA	22.6 ± 11.2	*n* = 8	11.5 ± 5.4	*n* = 6
Water	3.9 ± 3.8	*n* = 13	3.6 ± 1.8	*n* = 5

[a] For current recording, oocytes were voltage clamped to −60 mV by using two microelectrodes. The inward currents and the amplitudes of membrane depolarization induced by 10 mM nitrate, pH 5.5, are indicated.

[b] *n*, number of oocytes tested from five different frogs.

Expression Pattern of *AtNRT1:2* in Response to Nitrate Induction

The RNA gel blot analyses shown in Figure 4A demonstrate that like *CHL1*, *AtNRT1:2* is a root dominant gene. However,

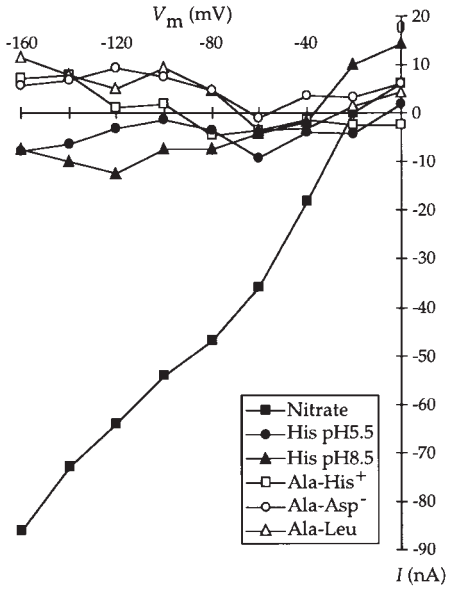

Figure 2. Current-to-Voltage Relationship Recorded in *AtNRT1:2*-Injected Oocytes.

Each *AtNRT1:2*-injected oocyte was exposed to 10 mM nitrate, pH 5.5 (filled squares); 10 mM dipeptides Ala-His$^+$ (open squares), Ala-Asp$^-$ (open circles), or Ala-Leu, pH 5.5 (open triangles); or 10 mM histidine, pH 5.5 (filled circles), or pH 8.5 (filled triangles). The oocyte was voltage clamped from −60 mV to a voltage between 0 and −160 mV for 300 msec with −20 mV increments. Currents (*I*) presented here are the difference between measurements conducted in the presence and absence of substrate. Currents elicited at the end of 300-msec pulses were plotted as the function of the voltage. Results obtained in three other oocytes isolated from two different frogs were similar. (+), positively charged; (−), negatively charged.

the expression patterns of *AtNRT1:2* and *CHL1* in response to nitrate induction are different. *CHL1* mRNA levels were low in ammonium-grown plants, peaked at 4 hr after nitrate induction, and then declined (Figure 4B). In contrast, *AtNRT1:2* mRNA levels were high in ammonium-grown plants (at 0 hr, row 1 of Figure 4B) and remained relatively constant during the time course of nitrate induction, except at 1 hr after induction. One hour after nitrate induction, the expression level of *AtNRT1:2* mRNA dropped, whereas that of *CHL1* mRNA started to increase significantly. In another independent experiment for nitrate induction, the *CHL1* mRNA level responded to nitrate more quickly by peaking at 2 hr after exposure to nitrate, and the *AtNRT1:2* mRNA level dropped earlier, at 0.5 hr after induction (Figure 4C).

Although the transient repression of *AtNRT1:2* mRNA and the increase in the levels of *CHL1* mRNA were temporally coupled in response to nitrate induction, it appears that the repression of *AtNRT1:2* mRNA was not a direct consequence of the increase of *CHL1* mRNA, because a persistent transient drop of *AtNRT1:2* mRNA in response to nitrate induction was observed in the *chl1* deletion mutant *chl1-5* (data not shown). It has been shown that the expression of *CHL1* is induced by acidic pH (Tsay et al., 1993). In comparison, a pH shift in the presence or absence of nitrate did not cause a significant change in the mRNA level of *AtNRT1:2* (data not shown), which is in keeping with its above-mentioned constitutive expression.

In Vivo Function of AtNRT1:2 Indicated by the Phenotypes of Transgenic Antisense *AtNRT1:2* Plants

To investigate the in vivo function of AtNRT1:2, antisense *AtNRT1:2* constructs were introduced into both wild-type and *chl1-5* plants. These transgenic plants were subjected to in vivo nitrate uptake assays and chlorate resistance tests. Chlorate is a nitrate analog that can be taken up by nitrate transporters and then reduced by nitrate reductase to chlorite, which is toxic. Therefore, mutants defective in nitrate uptake are expected to be more resistant to chlorate treatment. Indeed, two independent transgenic lines containing antisense *AtNRT1:2* in the *chl1-5* deletion background, designated As1 and As2, were more resistant to chlorate treatment than was the *chl1-5* mutant. As shown in Figure 5, two *chl1* mutants, *chl1-1* and *chl1-5*, were resistant to 2 mM chlorate but sensitive to 7 mM chlorate; in comparison, As1 and As2 were resistant to 7 mM chlorate.

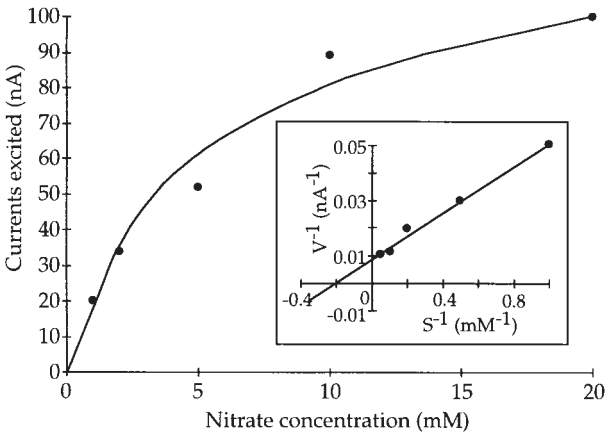

Figure 3. Kinetics of Nitrate-Elicited Currents in *AtNRT1:2*-Injected Oocytes.

Oocytes were voltage clamped at −60 mV. The currents elicited by nitrate, pH 5.5, in a single cRNA-injected oocyte were plotted as a function of external nitrate concentration. The inset shows a Lineweaver–Burk plot. The Lineweaver–Burk equation is $1/V = K_m/V_{max}[S] + 1/V_{max}$, where [*S*] is the nitrate concentration in mM, and *V* represents the current elicited in nA. The K_m value calculated by fitting the Lineweaver–Burk plot in this particular experiment is 5 mM. Similar analyses were performed in five independent oocytes, and the average K_m calculated was 5.9 ± 1.9 mM.

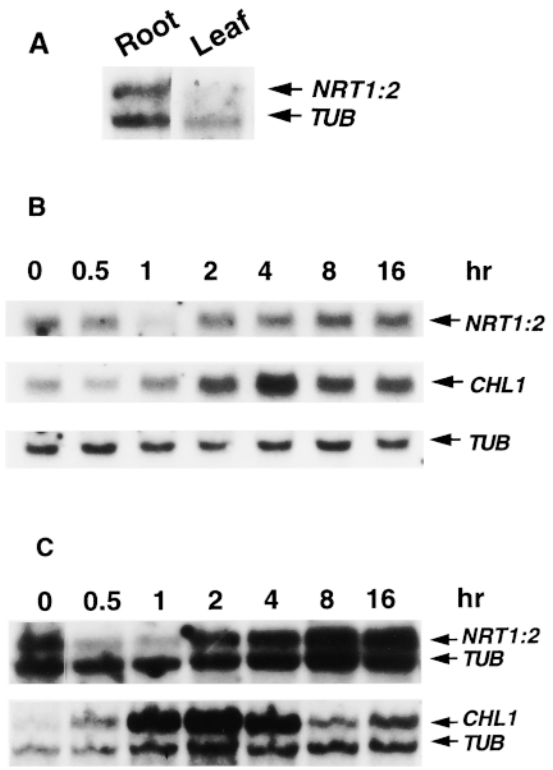

Figure 4. RNA Gel Blot Analysis of *AtNRT1:2* Expression.

(A) *AtNRT1:2* expression in root or leaf tissues.
(B) Time-course analysis of *AtNRT1:2* and *CHL1* mRNA levels following nitrate induction.
(C) Time-course analysis of *AtNRT1:2* and *CHL1* mRNA levels following nitrate induction in an independent experiment.
Total RNA (10 μg) was isolated from leaf or root tissues of plants grown on ammonium without nitrate for 2 weeks (0 hr) and then shifted to nitrate medium for 2 hr in **(A)** or for the time indicated above each lane in **(B)** and **(C)**. RNA was transferred to a Hybond N membrane (Amersham) and then hybridized with ^{32}P-radiolabeled DNA from *AtNRT1:2*, *CHL1*, and tubulin (*TUB*) genes.

This result provides further evidence for the involvement of AtNRT1:2 in nitrate uptake.

The As1 and As2 plants shown in Figure 5 belong to segregating T_1 progenies. Despite considerable effort and for reasons that are not clear, we could not obtain homozygous progeny from these two antisense lines. On the other hand, three homozygote transgenic plants containing antisense *AtNRT1:2* in the wild-type background were obtained. They were designated As3, As4, and As5 and used for in vivo uptake analyses. RNA gel blot analyses using these three transgenic plants and the antisense RNA probe *AtNRT1:2* showed a significant reduction in the levels of *AtNRT1:2* mRNA, which were only 34% (As3), 66% (As4), and 70% (As5) of the wild-type level. In comparison, the *AtNRT1:2* mRNA level in the *chl1-5* mutant was 94% that of the wild type (Figure 6A).

To determine whether antisense *AtNRT1:2* plants are defective in the cLATS, we investigated short-term nitrate uptake activity in noninduced plants by measuring membrane potentials in root epidermal cells of 6- to 7-day-old plants grown on ammonium without nitrate. As shown in Figure 7, when exposed to 10 mM nitrate, wild-type and transgenic plants all showed rapid membrane depolarizations, followed by a recovery of membrane potential, which is a characteristic electrophysiological response to nitrate that has been described for Arabidopsis (Meharg and Blatt, 1995; Wang and Crawford, 1996). In these antisense *AtNRT1:2* plants, nitrate-induced depolarizations were reduced to ~35% (As3), ~55% (As4), and ~60% (As5) of the amplitude found in wild-type plants (Figures 6B and 7A to 7D). Under the same conditions, depolarization observed in the *chl1-5* deletion mutant was ~80% of the wild-type level.

Consistent with the decreased depolarization in response to 10 mM nitrate, low-affinity nitrate uptake activities of 14-day-old antisense *AtNRT1:2* plants grown in ammonia without nitrate were reduced to 27% (As3), 30% (As4), and 56% (As5) that of the wild type (Figure 6C). Interestingly, there was a significant reduction of nitrate uptake activity in the *chl1-5* mutant (55% of the wild-type level) under the same conditions, and this reduction was larger than that observed for membrane depolarization (80% of the wild-type level). Three factors may contribute to the differences observed

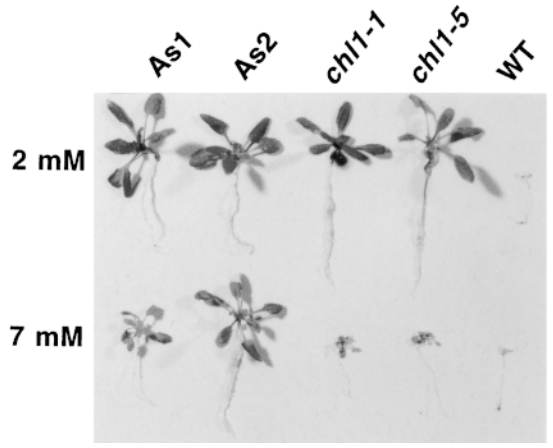

Figure 5. Chlorate Sensitivity Test of *chl1-5* Mutant and Transgenic Plants Expressing Antisense *AtNRT1:2* in the *chl1-5* Background.

Plants were treated with 2 mM (top) or 7 mM (bottom) chlorate at 3, 7, and 10 days after germination. Photographs were taken 7 days after the third treatment. *chl1-5* is a deletion mutant (Tsay et al., 1993) and *chl1-1* (originally named B1) is a *chl1* mutant isolated by Braaksma and Feenstra (1973); As1 and As2 are two independent transgenic plants containing antisense *AtNRT1:2* in a *chl1-5* mutant background. WT, wild type.

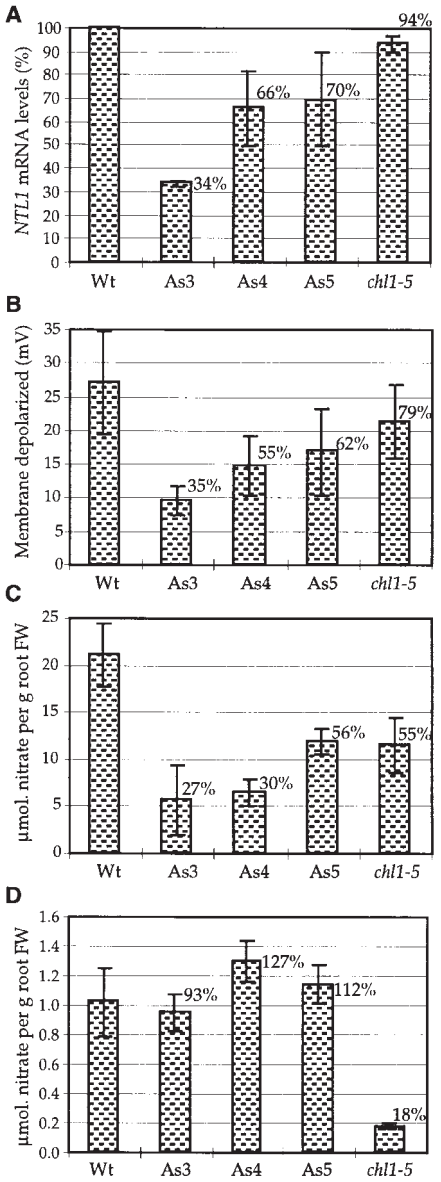

Figure 6. Defective Low-Affinity Nitrate Uptake Activities of Transgenic Plants Containing Antisense *AtNRT1:2*.

(A) *AtNRT1:2* mRNA levels of transgenic plants. Total RNA (10 μg) from roots of ammonium-grown plants was subjected to RNA gel blot analyses and hybridized with an antisense *AtNRT1:2* riboprobe or tubulin DNA probe. Quantification of the *AtNRT1:2* mRNA levels was based on densitometric measurements of the hybridization bands. The *AtNRT1:2* mRNA level was normalized with respect to the level of tubulin mRNA. Shown here are average percentages of wild-type (Wt) levels of *AtNRT1:2* mRNA determined from two to three experiments for each plant.

(B) Membrane depolarization responses to nitrate in root epidermal cells of wild-type and antisense *AtNRT1:2* plants. See Figure 7 legend for seedling growth and measurement. Shown here are average values of peak heights of depolarization observed in 20 wild-type, seven As3, 11 As4, 12 As5, and 11 *chl1-5* plants.

between the nitrate uptake assay and the membrane depolarization measurement, especially for the *chl1-5* mutant. (1) In mature roots, *CHL1* is primarily expressed in cortical or endodermal cells (Huang et al., 1996), whereas the membrane potentials were measured in epidermal cells. (2) The uptake assay was conducted with 14-day-old plants; the membrane potential was taken using 6- to 7-day-old plants. (3) The uptake assay was measured for a longer time after the shift to nitrate (30 min versus instantly for membrane depolarization).

To gauge the relative contribution of CHL1 and AtNRT1:2 to the LATS of Arabidopsis grown in different conditions, long-term (14 days) nitrate uptake activities of the wild type, the *chl1-5* deletion mutant, and the antisense As3 plant were measured and compared. The results showed that nitrate uptake activity of the *chl1* mutant was ~45% that of the wild type when plants were grown in KNO_3 and ~81% that of the wild type when they were grown in NH_4NO_3, whereas under the same conditions, the nitrate uptake activity of As3 was ~90% that of the wild type when plants were grown in KNO_3 and ~80% that of the wild type when they were grown in NH_4NO_3 (Figure 8).

Very recently, Wang et al. (1998) and our group (Liu et al., 1999) have independently shown that the *chl1* mutant is defective in both low- and high-affinity nitrate uptake (also see Figure 6D). The in vivo uptake data presented in Figure 6D (no defect in high-affinity nitrate uptake for As3, As4, and As5 plants) indicate that in contrast to CHL1, AtNRT1:2 is involved in low-affinity but not high-affinity uptake of nitrate. These data are in accord with those obtained from the functional analyses of AtNRT1:2 in oocytes (Liu et al., 1999).

Tissue-Specific Expression Pattern of the *AtNRT1:2* Gene Is Consistent with a Role in Uptake

The spatial distribution of *AtNRT1:2* mRNA in root tissues was examined by using in situ hybridization to determine in which root cells *AtNRT1:2* is expressed. Plants were grown vertically on ammonium-containing plates for 2 weeks and then shifted to nitrate-containing plates for 16 hr. Sections

(C) Comparison of low-affinity nitrate uptake activities of antisense *AtNRT1:2* plants and wild-type plants. Nitrate uptake activity of ammonium-grown plants was determined with 5 mM KNO_3 for 30 min. Experiments were performed in triplicate.

(D) Comparison of high-affinity nitrate uptake activities of antisense *AtNRT1:2* and wild-type plants. Nitrate uptake activity of ammonium-grown plants was determined with 250 μM KNO_3 for 30 min. Experiments were performed in triplicate.

The number above each bar is the percentage of the wild-type level. Error bars represent standard deviations. FW, fresh weight.

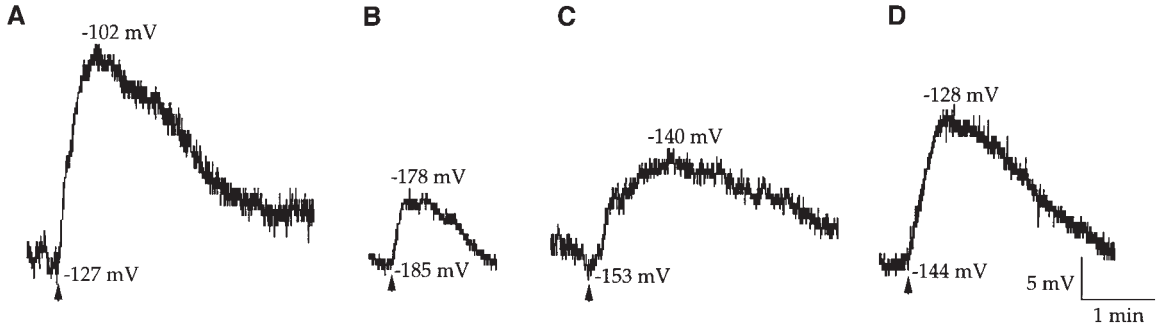

Figure 7. Membrane Potential Responses of Root Epidermal Cells to Nitrate Exposure.

(A) Response observed in the wild-type plant.
(B) Response observed in the transgenic As3 *AtNRT1:2* antisense plant.
(C) Response observed in the transgenic As4 *AtNRT1:2* antisense plant.
(D) Response observed in the transgenic As5 *AtNRT1:2* antisense plant.
Six- to 7-day-old seedlings grown on ammonium were bathed in a solution without nitrate. Arrowheads indicate when the seedlings were perfused with the same solution of 10 mM $CsNO_3$.

of the fixed root tissues were probed with ^{35}S-labeled antisense or sense transcripts of the *AtNRT1:2* cDNA. As shown in Figures 9A and 9B, a high density of silver grains (they appear yellow due to a colored filter) was found in epidermal cells and root hairs. This hybridization pattern was observed for sections of both mature roots (Figure 9) and young roots (i.e., regions close to the root tip; data not shown). As a control, similar sections were hybridized with the sense probe; in these controls, only a background level of signal in all layers of the root was found (Figures 9C and 9D). In Figure 9B, the signals found in vascular cylinders could be nonspecific due to the higher density of cells, because similar patterns also were observed in some of the control sections using the sense probe. These data indicate that *AtNRT1:2* mRNA accumulates primarily in the rhizodermis. The expression of *AtNRT1:2* in the rhizodermis is consistent with the notion that *AtNRT1:2* is directly involved in nitrate uptake.

DISCUSSION

Data from the present study strongly suggest that in addition to *CHL1*, *AtNRT1:2* is a low-affinity nitrate transporter directly involved in uptake. Furthermore, compared with previously reported properties of *CHL1* (Tsay et al., 1993; Huang et al., 1996), *AtNRT1:2* exhibits a number of distinct characteristics, indicating that it has unique functions in its own right.

In response to nitrate induction, the expression pattern of *AtNRT1:2* is different from that of *CHL1*. Whereas *CHL1* is a nitrate-inducible gene (Tsay et al., 1993), *AtNRT1:2* is constitutively expressed before plants are exposed to nitrate. Moreover, the expression level of *AtNRT1:2* remains relatively constant throughout the entire period of nitrate induction, except at the point at which the level of *CHL1* mRNA starts to increase significantly (Figures 4B and 4C). In light of the transient repression of *AtNRT1:2* mRNA, it appears that the process of constitutive low-affinity nitrate uptake is much more complex than was previously thought. However, for simplification and model interpretations, we can consider *AtNRT1:2* as a "constitutive" gene that encodes a cLATS component involved in nitrate uptake in Arabidopsis.

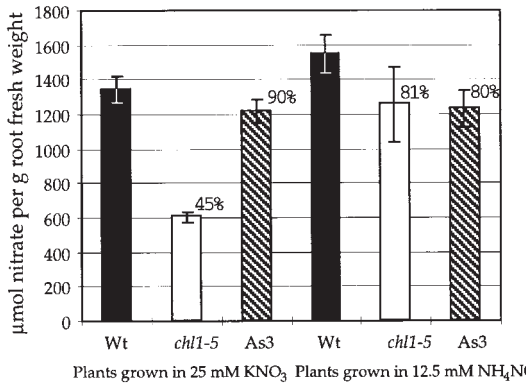

Figure 8. Long-Term (14 Days) Nitrate Uptake Activities of Wild-Type, *chl1-5*, and As3-Transgenic Plants.

Plants were germinated in a liquid medium containing 25 mM KNO_3 or 12.5 mM NH_4NO_3 as the nitrogen source and grown in continuous light. Fourteen days after germination, the amount of nitrate depleted from the medium was measured by HPLC analysis. Numbers above each bar are the percentage of the wild-type (Wt) level. Error bars represent standard deviations.

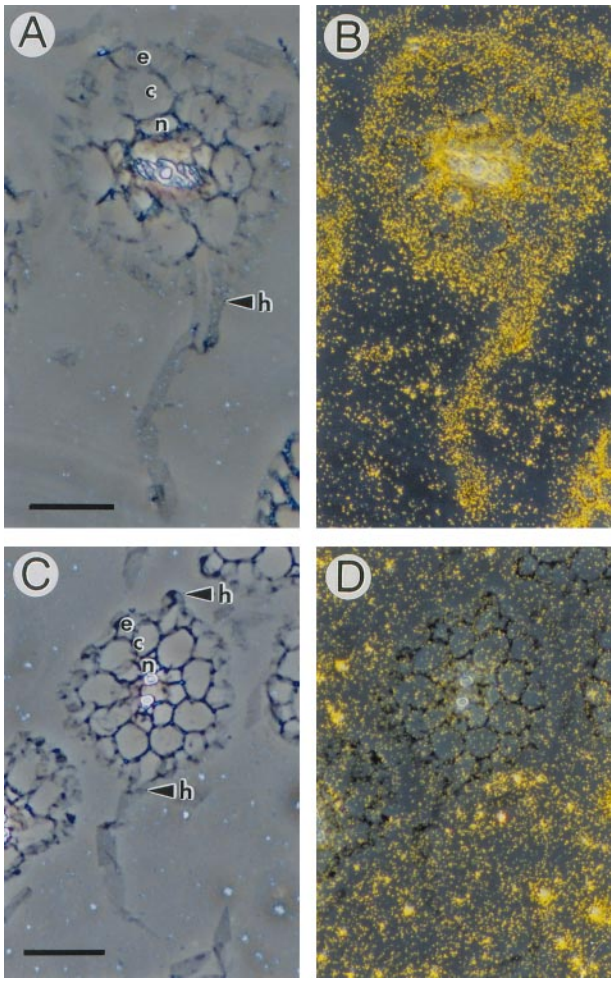

Figure 9. High Levels of *AtNRT1:2* mRNA Are Found in Root Epidermis and Root Hair.

(A) and **(B)** In situ hybridization of antisense *AtNRT1:2* probes to a cross-section of mature Arabidopsis root tissue. In **(A)**, bright-field microscopy was used. In **(B)**, double exposures using a colored filter for the dark-field exposure caused the *AtNRT1:2* signals to appear yellow.

(C) and **(D)** In situ hybridization of sense *AtNRT1:2* probes to a cross-section of mature Arabidopsis root tissue. For **(C)**, bright-field microscopy was used. In **(D)**, double exposures were taken, with a color filter for dark-field exposure.

c, cortical cells; e, epidermal cells; h, root hair; n, endodermal cells. Bars in **(A)** and **(C)** = 50 μm.

The spatial distribution of *AtNRT1:2* mRNA in root tissues is different from that of *CHL1*. The expression of *CHL1* changes basipetally, accumulating at high levels in the epidermal cells of young roots (root tip) and in endodermal and cortical cells of mature roots (Huang et al., 1996). The expression of *AtNRT1:2*, found primarily in rhizodermis (epidermis and hair; Figure 9), does not vary at different stages of root cell development. These data may suggest that for low-affinity nitrate transport in mature Arabidopsis roots, two different genes mediate uptake in the rhizodermis and in internal regions of the root (cortex and endodermis), respectively; that is, *CHL1* encodes an iLATS for the cortex and endodermis and *AtNRT1:2* encodes a cLATS for the rhizodermis.

The radial transport of ions taken up by rhizodermal cells is mediated mainly by the symplastic pathway. For ions to be taken up across the plasma membrane of the cortex or endodermis, the apoplastic pathway contributes to their radial transport driven by diffusion or mass flow to the free space (apoplasm) near these inner cells of roots. The relative contribution of the two pathways may depend on the preference of different ions, ion concentrations, apoplastic permeability, hydraulic conductivity of different root zones, and transpiration rates (Marschner, 1995). It is further possible that the transport of ions through the symplastic pathway competes with ions being metabolized by cytosolic enzymes or with ions being accumulated in vacuoles before they can be loaded into the xylem. These multiple possibilities suggest that the two pathways, which could be mediated separately by *CHL1* and *AtNRT1:2*, may complement each other to regulate the onset of nitrate storage, assimilation, and root–shoot partition under different growth conditions.

Analogous to the iHATS and the cHATS (Glass and Siddiqi, 1995), the two low-affinity transporters may also have somewhat different affinities and uptake capacities for nitrate. Unfortunately, our data could not conclusively determine which of the two has a higher affinity or capacity over the other. For example, the K_m values derived for AtNRT1:2 (5.9 ± 1.9 mM) and CHL1 (8.5 ± 3.1 mM; Huang et al., 1996) in Xenopus oocytes overlap with each other when standard deviations are taken into account. In terms of capacity, the relative contribution of *CHL1* and *AtNRT1:2* to LATS may change, depending on growth conditions. This is compounded by the fact that *AtNRT1:2* mRNA was not totally eliminated in the antisense *AtNRT1:2* plants (Figure 6A). Leaky expression of *AtNRT1:2* in the antisense plants and the fluctuation of expression of *CHL1* and *AtNRT1:2* under different growth conditions are two factors that may contribute to the following two observations.

First, in the presence of 2.5 mM NH_4NO_3, As3 plants were resistant to 0.8 mM chlorate but sensitive to 2 mM chlorate, whereas *chl1* plants were resistant to both concentrations of chlorate (data not shown). Second, compared with the wild type, the amount of nitrate taken up by *chl1* plants during long-term uptake experiments (14 days) was roughly 50% less when plants were grown in KNO_3 than when they were grown in NH_4NO_3 (Figure 8). This result supports our earlier speculation that a second LATS gene is more dominant than is *CHL1* when plants are grown in NH_4NO_3 (Huang et al., 1996). On the other hand, due to leaky expression of *AtNRT1:2*, the observed uptake activity (Figure 8) could neither substantiate nor disprove the hypothesis that *AtNRT1:2* is more dominant than is *CHL1* in NH_4NO_3-grown plants. In

addition, one cannot rule out the possibility that besides *CHL1* and *AtNRT1:2*, there is yet another transporter gene involved in LATS nitrate uptake.

Compared with other CHL1 homologs that have been demonstrated or believed to be nitrate transporters, the similarity between AtNRT1:2 and CHL1 is surprisingly low (36% identical, or approximately half the scores between CHL1 and its homologs from other plant species; see Figure 10). The low degree of similarity between AtNRT1:2 and CHL1 can be largely attributed to the long loop connecting the sixth and seventh putative transmembrane domains (Figure 1B). Our analysis from DNA gel blotting, searching EST databases, and deducing the amino acid sequences of three additional *CHL1* homologs besides *AtNRT1:2* (unpublished data) indicated that there are no genes in Arabidopsis that share a sequence identity >55% with *CHL1*.

Consistent with the two-component model, two *CHL1* homologs, one constitutive (*LeNRT1-1*) and one nitrate inducible (*LeNRT1-2*), were found in tomato (Lauter et al., 1996). *LeNRT1-1* and *LeNRT1-2* share 67% identity with *CHL1* and 88% with each other based on deduced amino acid sequence comparisons. Thus, it would seem that *LeNRT1-1* and *LeNRT1-2* are *CHL1* duplicates in tomato, whereas *CHL1* remains a single gene in Arabidopsis. Although the relatedness of *LeNRT1-1* and *LeNRT1-2* to *CHL1* (*AtNRT1*) at the level of in vivo functions is not clear, it is tempting to speculate that such a gene duplication is a characteristic of cultivars resulting from multiple crosses between closely related species. More perplexingly, the relationship between nitrate inducibility and mRNA localization of *LeNRT1-1* and *LeNRT1-2* is the opposite of that for *CHL1* and *AtNRT1:2*. *LeNRT1-1* is constitutive and expressed in both root hairs and other root fractions, whereas *LeNRT1-2* is nitrate inducible and preferentially expressed in root hairs (Lauter et al., 1996). In contrast, *CHL1* is nitrate inducible and expressed mainly in the inner layers of mature root (cortex and endodermis), whereas *AtNRT1:2* is constitutive and expressed primarily in root hairs and epidermis. The different distributions of inducible and constitutive transport systems seen in Arabidopsis and tomato might be a result of different adaptation processes among plants grown in natural ecosystems versus those that have been genetically improved for cultivation in arable soil, in which the nitrate concentration significantly fluctuates due to seasonal fertilization. Plant genome sequencing projects and cloning of more nitrate transporter genes should provide additional evidence to help elucidate these discrepancies between species.

The most striking difference between AtNRT1:2 and CHL1 is that whereas CHL1 is a dual-affinity nitrate transporter involved in both low- and high-affinity uptake of nitrate (Wang et al., 1998; Liu et al., 1999; Figure 6D), AtNRT1:2 appears to be a low-affinity nitrate transporter exhibiting no high-affinity nitrate uptake activity. Thus, in terms of nitrate affinity, nitrate regulation, and mRNA spatial distribution in root cells, *AtNRT1:2* differs significantly from *CHL1*. With its low degree of similarity to CHL1 (~36% amino acid identity; Figure 10), AtNRT1:2 may serve as a new probe to search for its own ortholog in other plant species.

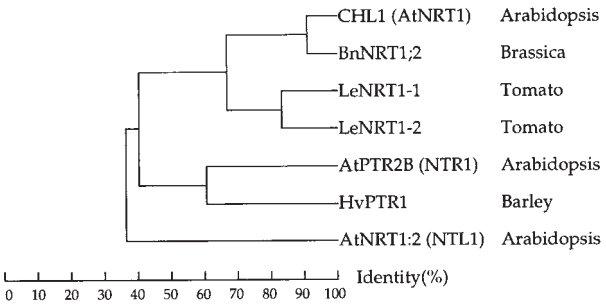

Figure 10. Phylogenetic Tree of CHL1 and Its Homologs in Higher Plants.

The phylogram was created using the Growtree program of the Genetics Computer Group package (version 9.1). BnNRT1;2 from Brassica (Muldin and Ingemarsson, 1995; Zhou et al., 1998) and LeNRT1-1 and LeNRT1-2 from tomato (Lauter et al., 1996) were cloned by hybridization to a *CHL1* cDNA probe. AtPTR2B (NTR1) is an Arabidopsis peptide transporter (Frommer et al., 1994; Rentsch et al., 1995; Song et al., 1996), and HvPTR1 is a barley peptide transporter (West et al., 1998). AtNRT1:2 is an Arabidopsis nitrate transporter described in this study.

METHODS

Isolation and Sequence Analysis of *AtNRT1:2* DNA

The expressed sequence tag (EST) clone p*AtNRT1:2-1* (clone YAP049) was obtained from the Nottingham Arabidopsis Stock Center (Nottingham, UK). The second cDNA clone, p*AtNRT1:2-2*, was isolated by screening an *Arabidopsis thaliana* cDNA library constructed in λYES vector (Elledge et al., 1991), using the insert of p*AtNRT1:2-1* as a probe. Both cDNA clones were subcloned into pBluescript II KS+ (Stratagene, La Jolla, CA) and sequenced by using the dideoxynucleotide chain termination method (Sanger et al., 1977) with the Sequenase kit (U.S. Biochemical).

Functional Expression of *AtNRT1:2* in Xenopus Oocytes

The insert of p*AtNRT1:2-1* was subcloned into pGEMHE, which contains 5′ and 3′ untranslated regions of the *Xenopus laevis* β-globin gene (Liman et al., 1992) to enhance protein expression in oocytes. Capped mRNA was transcribed from the linearized plasmid in vitro by using mMESSAGE mMACHINE kits (Ambion, Austin, TX). Oocytes were isolated and injected with 50 ng of complementary RNA (cRNA), as described previously (Tsay et al., 1993). For the current measurements, oocytes were voltage clamped to −60 mV using two microelectrodes and perfused initially with a solution containing 230 mM mannitol, 0.15 mM $CaCl_2$, and 10 mM Hepes, pH 7.4, and then with 220 mM mannitol, 0.15 mM $CaCl_2$, 10 mM Hepes, pH 5.5, plus $CsNO_3$ or Gly-Gly at the concentrations indicated. Oocytes were

initially perfused with a solution of pH 7.4 because oocytes are more stable at pH 7.4, and there was no leaking current when the external solution was changed from pH 7.4 to 5.5 in the absence of nitrate. Solutions used for the measurements of current-to-voltage curves were (1) 230 mM mannitol, 0.15 mM $CaCl_2$, and 10 mM Tris-Mes at different ratios to give rise to the pH indicated and (2) 220 mM mannitol, 0.15 mM $CaCl_2$, and 10 mM Tris-Mes at the pH indicated plus 10 mM HNO_3, histidine, or dipeptide. The ratio of Tris to Mes was adjusted to arrive at each of the desired pH values of the solution. Measurements were recorded by a 486-based microcomputer using the AXOTAPE and pCLAMP program (Axon Instruments, Inc., Foster City, CA).

RNA Gel Blot Analysis

Plants were grown vertically on agarose plates with 12.5 mM $(NH_4)_2$-succinate and 0.45% agarose (FMC, Rockland, ME), pH 6.5, for 14 days, as previously described (Tsay et al., 1993), and then shifted to plates with 25 mM KNO_3 as a nitrogen source at pH 5.5 for the time points indicated. Our previous experiments indicated that when nitrate was the sole nitrogen source, 5.5 was the optimal pH for plant growth, whereas when ammonium was the sole nitrogen source, 6.5 was the optimal pH. However, after 14 days of plant growth, the pH of the ammonium medium, due to ammonium uptake, was significantly altered, from 6.5 to ~5.7 to 5.8. Therefore, the plants did not experience a dramatic pH change during the shift to KNO_3 medium at pH 5.5. Furthermore, the choice of 25 mM and not a micromolar nitrate concentration in these expression experiments was to avoid ambiguities that might arise because AtNRT1:2 is a low-affinity transporter.

Total RNA from root tissues was isolated by TRIzol reagent (Gibco BRL, Grand Island, NY). Hybridization was performed at 68°C in 5 × SSPE (1 × SSPE is 0.15 M NaCl, 10 mM sodium phosphate, and 1 mM EDTA), 5 × Denhardt's solution (1 × Denhardt's solution is 0.02% Ficoll, 0.02% PVP, and 0.02% BSA), 5% (w/v) dextran sulfate, 0.5% SDS, and 25 μg/mL salmon sperm DNA. The 1.5 kb of the 5′ portion of the *AtNRT1:2* cDNA was used to synthesize the DNA or RNA probe for RNA gel blot analyses. Membranes were washed with 2 × SSPE at room temperature for 20 min, 2 × SSPE and 0.5% SDS at 68°C for 30 min, and 0.2 × SSPE and 0.5% SDS at 68°C for 30 min and then briefly rinsed with 2 × SSPE at room temperature.

Plant Transformation

To obtain plants expressing *AtNRT1:2* in an antisense orientation, the 1.5-kb 5′ portion of the *AtNRT1:2* cDNA was inserted between the cauliflower mosaic virus 35S promoter and the nopaline synthase terminator in the opposite orientation and then subcloned into the binary vector pBIN19 to produce the plasmid pAntisense (As)–*AtNRT1:2*. The pAs–*AtNRT1:2* construct was introduced into wild-type and *chl1-5* plants by using *Agrobacterium tumefaciens*–mediated in-the-plant vacuum infiltration (Bechtold et al., 1993). Transformants were confirmed by kanamycin resistance and genomic DNA gel blot analyses. Two independent transgenic plants in the *chl1-5* background (As1 and As2) were used for the chlorate resistance test, and homozygote progenies of three independent transgenic plants in the wild type (As3, As4, and As5) were used for nitrate uptake assays. There were two copies of the insert in As2, As3, and As 4, three in As1, and six in As5.

Chlorate Sensitivity Assay

Seeds were sown in pots containing vermiculite and Perlite (South Sea Vermiculite and Perlite Co., Taipei, Taiwan) mixed at a 2:1 ratio and wetted with a nutrient solution containing 2.5 mM NH_4NO_3 (Wilkinson and Crawford, 1991). After a 3-day vernalization treatment at 4°C, the pots were moved to a 24°C growth chamber with continuous light. Nutrient solutions containing 0.8, 2, or 7 mM chlorate were applied at 3, 7, and 10 days after germination.

Nitrate-Induced Membrane Depolarization of Arabidopsis Roots

Plants were grown vertically on agarose plates with 12.5 mM $(NH_4)_2$-succinate and 0.45% agarose (FMC), pH 6.5, as described previously (Tsay et al., 1993), for 6 to 7 days. At this stage, the root length was ~2 to 2.5 cm. For recording, seedlings were transferred to a narrow chamber of 0.3 cm^3 and perfused with a bath solution of 1 mM Mes, pH 5.5, 0.25 mM KCl, and 1 mM $CaCl_2$ at 2.5 mL min^{-1}. A micropipette pulled from filamented borosilicate glass capillaries with a tip diameter of ~250 nm was filled with 200 mM KCl and used to impale root epidermal cells 0.5 to 1 cm from the root tip by attaching the pipette to the root surface and then tapping the micromanipulator that held the micropipette. Six- to 7-day-old plants were used for the measurements due to the low activity found in younger plants and the difficulty of impaling older plants (Meharg and Blatt, 1995; Wang and Crawford, 1996; Y.-F. Tsay, unpublished data). Cells with membrane potentials in the range from −120 to −190 mV were selected for further analyses.

Nitrate Uptake Assay of Arabidopsis Plants

Approximately 30 seeds were surface sterilized, sown in 125-mL flasks containing 25 mL of liquid medium with 10 mM K_2HPO_4, 2 mM $MgSO_4$, 0.1 mM $FeSO_4$-EDTA, 1 mM $CaCl_2$, 50 μM H_3BO_3, 12 μM $MnSO_4 \cdot H_2O$, 1 μM $ZnCl_2$, 1 μM $CuSO_4 \cdot 5H_2O$, 0.2 μM $Na_2MoO_4 \cdot 2H_2O$, 1 mg/L thiamin, 100 mg/L inositol, 0.5 mg/L pyridoxine, 0.5 mg/L nicotinic acid, 1 g/L Mes, 0.5% sucrose, and 12.5 mM $(NH_4)_2$-succinate as the sole nitrogen source at pH 6.5. Plants were grown under continuous illumination at 24°C and rotated at 80 rpm. Fourteen-day-old plants were washed twice with 5 mM K_2HPO_4/KH_2PO_4, pH 5.5, and then shifted to 11 mL of the liquid medium described above, with either 5 mM KNO_3 or 250 μM KNO_3, pH 5.5. Nitrate uptake activities were determined as the amount of nitrate depleted from the medium during a 30-min period by HPLC (Thayer and Huffaker, 1980), using a PARTISIL 10 SAX (strong anion exchange) column (Whatman, Clifton, NJ). Plants were blotted dry, and fresh weights were measured immediately after the last sample was taken. For long-term uptake measurement, 30 plants were grown with 25 mL of 25 mM KNO_3 or 12.5 mM NH_4NO_3, pH 5.5, for 14 days, and then the amounts of nitrate depleted from the medium were determined by HPLC analysis.

In Situ Hybridization

Plants were grown vertically on agarose nutrient plates containing 12.5 mM $(NH_4)_2$-succinate, pH 6.5, for 14 days and then shifted to 25 mM KNO_3-containing plates, pH 5.5, for 16 hr. The roots were cut into small pieces (<4 mm long) in a fixative mix (50% ethanol, 5.0% acetic acid, and 3.7% formaldehyde), placed twice under a vacuum

for 15 min each, and then incubated at room temperature for an additional 2 hr. The specimens were then dehydrated in various concentrations of ethanol (50, 70, 95, and 100%) and incubated three times for 30 min at each concentration. After overnight incubation in 95 or 100% ethanol, the specimens were embedded as follows: 100% ethanol–xylene (1:1) for 30 min; pure xylene for 15 min, twice; xylene–melted Paraplast (Oxford, St. Louis, MO) (3:1, 1:1, and 1:3) at 62°C for 30 min each; and pure melted Paraplast (Oxford) at 62°C for 1 hr, three times. Finally, the tissues that were embedded in the desired orientation were cut into 8-μm sections. ^{35}S-labeled *AtNRT1:2* antisense and sense RNA probes were synthesized using T3 or T7 RNA polymerase from EcoRI- or SalI-linearized pBluescript II KS+ *AtNRT1:2* cDNA clones in which 0.5 kb of the 3′ end and the poly(A) tail had been eliminated. Root sections were hybridized with hydrolyzed RNA probes and washed as previously described (Jackson, 1991; McKhann and Hirsch, 1993). Slides were exposed for 65 days.

ACKNOWLEDGMENTS

We thank the Nottingham Arabidopsis Stock Center for providing the EST clone YAPO49, Dr. Choun-Sea Lin for his help in the preparation of photographs, and Dr. Nigel Crawford for helpful discussions. This work was supported by grants from Academia Sinica and the National Science Council of Taiwan (No. NSC-86-2311-B001-011 and No. NSC-87-2311-B001-077).

Received January 5, 1999; accepted May 14, 1999.

REFERENCES

Aslam, M., Travis, R.L., and Huffaker, R.C. (1992). Comparative kinetics and reciprocal inhibition of nitrate and nitrite uptake in roots of uninduced and induced barley (*Hordeum vulgare* L.) seedlings. Plant Physiol. **99,** 1124–1133.

Bechtold, N., Ellis, J., and Pelletier, G.C.R. (1993). *In planta Agrobacterium*–mediated gene transfer by infiltration of adult *Arabidopsis thaliana* plants. C. R. Acad. Sci. Ser. III Sci. Vie **316,** 1194–1199.

Behl, R., Tichner, R., and Raschke, K. (1988). Induction of a high-capacity nitrate-uptake mechanism in barley roots prompted by nitrate uptake through a constitutive low-capacity mechanism. Planta **176,** 235–240.

Boorer, K.J., Loo, D.D.F., and Wright, E.M. (1994). Steady-state and presteady-state kinetics of the H^+/hexose cotransporter (STP1) from *Arabidopsis thaliana* expressed in *Xenopus* oocytes. J. Biol. Chem. **269,** 20417–20424.

Boorer, K.J., Frommer, W.B., Bush, D.R., Kreman, M., Loo, D.D.F., and Wright, E.M. (1996). Kinetics and specificity of a H^+/amino acid transporter from *Arabidopsis thaliana*. J. Biol. Chem. **271,** 2213–2220.

Braaksma, F.J., and Feenstra, W.J. (1973). Isolation and characterization of chlorate-resistant mutants of *Arabidopsis thaliana*. Mutat. Res. **19,** 175–185.

Crawford, N.M., and Glass, A.D.M. (1998). Molecular and physiological aspects of nitrate uptake in plants. Trends Plant Sci. **3,** 389–395.

Daniel-Vedele, F., Filleur, S., and Caboche, M. (1998). Nitrate transport: A key step in nitrate assimilation. Curr. Opin. Plant Sci. **1,** 235–239.

Doddema, H., and Telkamp, G.P. (1979). Uptake of nitrate by mutants of *Arabidopsis thaliana*, disturbed in uptake or reduction of nitrate. Physiol. Plant. **45,** 332–338.

Doddema, H., Hofstra, J.J., and Feenstra, W.J. (1978). Uptake of nitrate by mutants of *Arabidopsis thaliana*, disturbed in uptake or reduction of nitrate. I. Effect of nitrogen source during growth on uptake of nitrate and chlorate. Physiol. Plant. **43,** 343–350.

Elledge, S.J., Mulligan, J.T., Ramer, S.W., Spottswood, M., and Davis, R.W. (1991). λYES: A multifunctional cDNA expression vector for the isolation of genes by complementation of yeast and *Escherichia coli* mutations. Proc. Natl. Acad. Sci. USA **88,** 1731–1735.

Frommer, W.B., Hummel, S., and Rentsch, D. (1994). Cloning of an *Arabidopsis* histidine transporting protein related to nitrate and peptide transporters. FEBS Lett. **347,** 185–189.

Glass, A.D.M., and Siddiqi, M.Y. (1995). Nitrogen absorption by plant roots. In Nitrogen Nutrition in Higher Plants, H.S. Srivastava and R.P. Singh, eds (New Delhi: Associated Publishing Co.), pp. 21–56.

Goyal, S.S., and Huffaker, R.C. (1986). A novel approach and a fully automated microcomputer-based system to study kinetics of NO_3^-, NO_2^-, and NH_4^+ transport simultaneously by intact wheat seedlings. Plant Cell Environ. **9,** 209–215.

Hole, D.J., Emran, A.M., Fares, Y., and Drew, M. (1990). Induction of nitrate transport in maize roots, and kinetics of influx, measured with nitrogen-13. Plant Physiol. **93,** 642–647.

Hopp, T.P., and Woods, K.R. (1981). Prediction of protein antigenic determinants from amino acid sequences. Proc. Natl. Acad. Sci. USA **78,** 3824–3828.

Huang, N.-C., Chiang, C.-S., Crawford, N.M., and Tsay, Y.-F. (1996). *CHL1* encodes a component of the low-affinity nitrate uptake system in Arabidopsis and shows cell type–specific expression in roots. Plant Cell **8,** 2183–2191.

Jackson, D. (1991). *In situ* hybridization in plants. In Molecular Plant Pathology: A Practical Approach, D.J. Bowles, S.J. Gurr, and M. McPhereson, eds (Oxford, UK: Oxford University Press), pp. 163–174.

Krapp, A., Fraisier, V., Scheible, W., Quesada, A., Gojon, A., Stitt, M., Caboche, M., and Daniel-Vedele, F. (1998). Expression studies of *Nrt2:1Np*, a putative high-affinity nitrate transporter: Evidence for its role in nitrate uptake. Plant J. **14,** 723–731.

Lauter, F.-R., Ninnemann, O., Bucher, M., Riesmeier, J.W., and Frommer, W.B. (1996). Preferential expression of an ammonium transporter and of two putative nitrate transporters in root hairs of tomato. Proc. Natl. Acad. Sci. USA **93,** 8139–8144.

Lee, R.B., and Drew, M.C. (1986). Nitrogen-13 studies of nitrate fluxes in barley roots. II. Effect of plant N-status on the kinetic parameters of nitrate influx. J. Exp. Bot. **185,** 1768–1779.

Liman, E.R., Tytgat, J., and Hess, P. (1992). Subunit stoichiometry of a mammalian K^+ channel determined by construction of multimeric cDNAs. Neuron **9,** 861–871.

Liu, K.-H., Huang, C.-Y., and Tsay, Y.-F. (1999). CHL1 is a dual-affinity nitrate transporter of Arabidopsis involved in multiple phases of nitrate uptake. Plant Cell **11,** 865–874.

Mackenzie, B., Loo, D.D.F., Fei, Y.-J., Liu, W., Ganapathy, V., Leibach, F.H., and Wright, E.M. (1996). Mechanisms of the human intestinal H^+-coupled oligopeptide transporter hPEPT1. J. Biol. Chem. **271,** 5430–5437.

Marschner, H. (1995). Mineral Nutrition of Higher Plants. (London: Academic Press).

McKhann, H.I., and Hirsch, A.M. (1993). *In situ* localization of specific mRNAs in plant tissues. In Methods in Plant Molecular Biology and Biotechnology, B.R. Glick and J.E. Thompson, eds (Boca Raton, FL: CRC Press), pp.179–205.

Meharg, A.A., and Blatt, M.R. (1995). NO_3^- transport across the plasma membrane of *Arabidopsis thaliana* root hairs: Kinetic control by pH and membrane voltage. J. Membr. Biol. **145,** 49–66.

Muldin, I., and Ingemarsson, B. (1995). A cDNA from *Brassica napus* L. encoding a putative nitrate transporter. Plant Physiol. **108,** 1341.

Paulsen, I.T., and Skurray, R.A. (1994). The POT family of transport proteins. Trends Biol. Sci. **19,** 404.

Quesada, A., Krapp, A., Trueman, L.J., Daniel-Vedele, F., Fernandez, E., Forde, B.G., and Caboche, M. (1997). PCR-identification of a *Nicotiana plumbaginifolia* cDNA homologous to the high-affinity nitrate transporters of the *crnA* family. Plant Mol. Biol. **34,** 265–274.

Rentsch, D., Laloi, M., Rouhara, I., Schmelzer, E., Delrot, S., and Frommer, W.B. (1995). *NTR1* encodes a high affinity oligopeptide transporter in Arabidopsis. FEBS Lett. **370,** 264–268.

Sanger, F., Nicklen, S., and Coulson, A.R. (1977). DNA sequencing with chain terminating inhibitors. Proc. Natl. Acad. Sci. USA **74,** 5463–5467.

Siddiqi, M.Y., Glass, A.D.M., Ruth, T.J., and Rufty, J.T.W. (1990). Studies of the uptake of nitrate in barley. Plant Physiol. **93,** 1426–1432.

Song, W., Steiner, H.-Y., Zhang, L., Naider, F.G.S., and Becker, J.M. (1996). Cloning of a second Arabidopsis peptide transport gene. Plant Physiol. **110,** 171–178.

Steiner, H.-Y., Naider, F., and Becker, J.M. (1995). The PTR family: A new group of peptide transporters. Mol. Microbiol. **16,** 825–834.

Thayer, J.R., and Huffaker, R.C. (1980). Determination of nitrate and nitrite by high-pressure liquid chromatography: Comparison with other methods for nitrate determination. Anal. Biochem. **102,** 110–119.

Touraine, B., and Glass, A.D.M. (1997). NO_3^- and ClO_3^- fluxes in the *chl1-5* mutant of *Arabidopsis thaliana*. Plant Physiol. **114,** 137–144.

Trueman, L.J., Onyeocha, I., and Forde, B.G. (1996a). Recent advances in the molecular biology of a family of eukaryotic high affinity nitrate transporters. Plant Physiol. Biochem. **34,** 621–627.

Trueman, L.J., Richardson, A., and Forde, B.G. (1996b). Molecular cloning of higher plant homologues of the high-affinity nitrate transporters of *Chlamydomonas reinhardtii* and *Aspergillus nidulans*. Gene **175,** 223–231.

Tsay, Y.-F., Schroeder, J.I., Feldmann, K.A., and Crawford, N.M. (1993). The herbicide sensitivity gene *CHL1* of Arabidopsis encodes a nitrate-inducible nitrate transporter. Cell **72,** 705–713.

Wang, R., and Crawford, N.M. (1996). Genetic identification of a gene involved in constitutive, high-affinity nitrate transport in higher plants. Proc. Natl. Acad. Sci. USA **93,** 9297–9301.

Wang, R., Liu, D., and Crawford, N.M. (1998). The *Arabidopsis* CHL1 protein plays a major role in high-affinity nitrate uptake. Proc. Natl. Acad. Sci. USA **95,** 15134–15139.

Werf, A.V.D., Raaimakers, D., Poot, P., and Lambers, H. (1988). Respiratory energy costs for the maintenance of biomass, for growth and for iron uptake in roots of *Carex diandra* and *Carex acutiformis*. Physiol. Plant. **72,** 483–491.

West, C.E., Waterworth, W.M., Stephens, S.M., Smith, C.P., and Bray, C.M. (1998). Cloning and functional characterization of a peptide transporter expressed in the scutellum of barley grain during the early stages of germination. Plant J. **15,** 221–229.

Wilkinson, J.Q., and Crawford, N.M. (1991). Identification of the Arabidopsis *CHL3* gene as the nitrate reductase structural gene *NIA2*. Plant Cell **3,** 461–471.

Wirén, N., Gazzarrini, S., and Frommer, W.B. (1997). Regulation of mineral nitrogen uptake in plants. Plant Soil **196,** 191–199.

Yamashita, T., Shimada, S., Guo, W., Sato, K., Kohmura, E., Hayakawa, T., Takagi, T., and Tohyama, M. (1997). Cloning and functional expression of a brain peptide/histidine transporter. J. Biol. Chem. **272,** 10205–10211.

Zhou, J.-J., Theodoulou, F.L., Muldin, I., Ingemarsson, B., and Miller, A.J. (1998). Cloning and functional characterization of a *Brassica napus* transporter that is able to transport nitrate and histidine. J. Biol. Chem. **273,** 12017–12023.